

Acanthopanax Cortex extract: A novel photosensitizer for head and neck squamous cell carcinoma therapy

Shuhan Shi^{a,b,1}, Hyejeoung Cho^{a,1}, Qiaochu Sun^a, Yuzhu He^a, Guowu Ma^b, Young Kim^a,
Byunggook Kim^c, Okjoon Kim^{a,*}

^a Department of Oral Pathology, Dental Science Research Institute, School of Dentistry, Chonnam National University, Gwangju, 61186, Republic of Korea

^b Department of Oral Maxillofacial Surgery, College of Stomatology, Dalian Medical University, Dalian 116044, China

^c Department of Oral Medicines, School of Dentistry, Chonnam National University, Gwangju 61189, Republic of Korea

ARTICLE INFO

Keywords:

Head and neck squamous cell carcinoma
Photodynamic therapy
Natural photosensitizer
Acanthopanax Cortex
Apoptosis

ABSTRACT

Objectives: The aim of this study was to develop a novel photosensitizer from traditional plant extracts and to investigate the photodynamic therapy (PDT) effect and mechanism of action of the novel photosensitizer on KB and Hep-2 cells.

Methods: Fluorescence emission, cell viability, and intracellular distribution of candidates were analyzed to screen potential photosensitizers from traditional plant extracts. Cellular reactive oxygen species (ROS) quantification, Annexin V-FITC/PI staining, and western blotting were performed to explore the mechanism of cell death in KB and Hep-2 cells.

Result: Of 289 traditional plant extracts, 13 plant extracts with strong fluorescence were initially screened by fluorescence emission analysis. The cell viability assay and intracellular distribution of candidates showed that *Acanthopanax Cortex* (AC) extract is a potential photosensitizer. Under optimal PDT conditions, high levels of ROS were produced in KB and Hep-2 cells, followed by cell death. However, there was no significant damage to HaCaT cells. Moreover, apoptosis induced by AC extract with 625 nm irradiation (IR) down-regulated the expression of Bcl-2 protein and up-regulated the expression of Bax protein, as well as that of cleaved PARP-1 protein in both KB and Hep-2 cells.

Conclusion: The fluorescence intensity of AC extract at 420 nm is similar to that of the commercial Hematoporphyrin (HP). AC extract with 625 nm IR could enhance the PDT effect, induce ROS generation, and trigger apoptotic pathways in KB and Hep-2 cells. Therefore, we suggest that AC is a potential novel photosensitizer for PDT in head and neck squamous cell carcinoma.

1. Introduction

Head and neck squamous cell carcinoma (HNSCC) is the seventh most common cancer in the world, accounting for 5% of global cancer [1]. The cancerous tissue develops mainly in the mouth, nose, and throat. Although the main treatments include surgery, radiation therapy, chemotherapy, immunotherapy, or a combination of these [2,3], photodynamic therapy (PDT) has become a clinically approved and minimally invasive treatment, which is gradually becoming a mainstream cancer treatment [4]. After PDT, the complete remission rate of early laryngeal cancer and precancerous lesions was 77.6% (249/321); the therapeutic effect of PDT on recurrent laryngeal papillomatosis has also been previously observed [5].

The treatment principle of PDT is that, when irradiated with light of a particular wavelength, the photosensitizer undergoes a transition to react with endogenous oxygen to produce singlet oxygen and other free radicals, resulting in rapid and selective destruction of the target tissue [6]. Therefore, selection of the photosensitizer is a critical aspect of the therapy. The ideal photosensitizer should be non-toxic and only show local toxicity after activation by light [7]. Many kinds of photosensitizers have been developed and commercially used, such as hematoporphyrin derivatives, chlorins, and phthalocyanines [8–10]. Although they have been used for many years in clinical setting, the limitations of these photosensitizers cannot be ignored. Studies have shown that photofrin-related photosensitizers are excreted slowly after entering the body and can sensitize the skin [11,12]. Hematoporphyrin

* Corresponding author.

E-mail address: js3894@jnu.ac.kr (O. Kim).

¹ These authors contributed equally to this work.

monomethyl ether has low light absorbance and forms aggregates in solution, which also hinders its clinical application [13]. Exploring more efficient and safer photosensitizers is a new challenge; traditional plants could be a potential source for such photosensitizers. The number of novel chemicals obtained from natural products is generally higher than that obtained synthetically, making natural ingredients a useful resource for the development of new drugs [14]. Recently, some traditional plants have been studied as photosensitizers. For example, curcumin combined with nano-liposomes for PDT in HepG-2 tumor model produced a good tumor regression effect [15]. Aloe emodin was used as a photosensitizer to confirm its inhibitory effect on oral mucosal carcinoma and human gastric cancer [16,17]. The activation of natural photosensitizers with light of specific wavelength settings should be considered in PDT. One study has shown that red and infrared radiation, including red light wavelengths of 620–670 nm, can penetrate to greater depths in the tissue [18]. In some reports, 625 nm red light effectively assists in the treatment of various cancers [19,20]. Based on this, there may be potential photosensitizers that can be activated by 625 nm red light in traditional plants.

In this study, 13 of 289 traditional plant extracts tested showed strong fluorescence intensities comparable to those of the commercial photosensitizer HP. *Acanthopanax Cortex* (AC) and *Houttuyniae Herba* (HH) extracts significantly induced cell death under 625 nm IR treatment. In particular, AC extract showed less cell toxicity in normal keratinocyte HaCaT cells than HH extract under PDT conditions. Therefore, we suggest that AC extract could be used as a potential photosensitizer for further experiments in HNSCC therapy.

2. Materials and methods

2.1. Fluorescence emission analysis

We purchased 289 traditional plant extracts from the Korea Plant Extract Bank (Ochang, Korea). Every plant extract was prepared in dimethyl sulfoxide (DMSO; JUNSEI, Tokyo, Japan) at a concentration of 500 µg/ml. Hematoporphyrin (HP; Sigma-Aldrich, St. Louis, USA) was also prepared in dimethyl sulfoxide (DMSO; Calbiochem, Burlington, USA) at concentrations of 1–500 µg/ml. Fluorescence measurement was performed with an FL X800 microplate fluorescence reader (BioTek Instruments, Vermont, USA) using 500 µg/ml of the plant extracts and HP (Excitation: 420/50 nm; Emission: 645/40 nm).

2.2. Cell culture

Human laryngeal epithelial cancer cells (KB and Hep-2 cells) were purchased from the Korea Cell Line Bank (Seoul, South Korea). KB cells of this line contain HeLa marker chromosomes and were derived via HeLa contamination. Human keratinocyte HaCaT cells were obtained from the Korea Institute of Oriental Medicine (Deajeon, South Korea). HaCaT cells are a spontaneously immortalized, human keratinocyte line that has been widely used for the studies of skin biology and differentiation [21]. HaCaT cells were used as the normal cell in this study. All cell lines were maintained in Dulbecco's modified eagle's medium (DMEM; WELGENE, Gyeongsan, South Korea) containing 10% heat-inactivated fetal bovine serum (FBS; JR Scientific, Woodland, USA), and antibiotic antimycotic solution (AA; WELGENE) in a humidified atmosphere of 5% CO₂ at 37 °C.

2.3. Irradiation conditions

A continuous-wavelength light-emitting diode (LED) with a wavelength of 625 nm at a power density of 1 mW/cm² (3.6 J/cm²) was used for PDT. There is a study that showed that aloe emodin combined with 3.2 J/cm² of light energy can inhibit oral mucosal carcinoma [16]. Another study showed that 1 h of 625 nm LED light source at 1 mW/cm² can trigger a natural photosensitizer to induce ROS generation in

Fadu cells [22]. As shown in supplementary data 1 (S1), the LED irradiation instrument (Department of Oral Pathology Chonnam National University, Gwangju, South Korea) was constructed in a humidified atmosphere of 5% CO₂ at 37 °C. Each experimental group was irradiated for 1 h.

2.4. Preparation of extract solutions

Plant extract solutions were prepared in DMSO (20 mg/ml). The solutions were incubated overnight and then diluted in DMEM (0–500 µg/ml).

2.5. Cell viability assay

The PDT effects of traditional plant extracts were investigated by quantifying cell viability, with or without 625 nm IR conditions. KB, Hep-2, and HaCaT cells were seeded and cultured at a density of 1×10^5 /ml cell in 96-well plates. After 24 h, extracts were added to each well at various concentrations for a range of time periods (0–500 µg/ml for 0–12 h). After treatment, the culture dish was irradiated with 625 nm IR for 1 h. Then, the cells were cultured for 12 h. For the cell viability assay, the cells were washed twice with phosphate-buffered saline (PBS), and then 100 µl of 3-[4,5-dimethylthiazol-2-yl]-2,5-diphenyltetrazolium bromide (MTT; Sigma-Aldrich) was added to each well. After incubation for 3 h at 37 °C, MTT solution was discarded, 100 µl of DMSO was added to each well, and the plate was read at a wavelength of 570 nm using a microplate reader (BIO-RAD, CA, USA).

2.6. Determination of the intracellular distribution of AC extract

To investigate the intracellular distribution of AC extract, its fluorescence was visualized using a digital microscope (CELENA[®]S Digital Imaging System, Anyang, South Korea). KB and Hep-2 cells were grown on coverslips and incubated in DMEM containing 60 µg/ml AC extract for the indicated time (0–12 h). After incubation, the cells were treated with 4% formaldehyde fixative solution (T&I Co., Gwangju, Korea) for 5 min and washed twice with PBS. Then, cells were examined after incubation with 0.1 mg/ml 4',6-diamidino-2-phenylindole dihydrochloride (DAPI; Sigma-Aldrich) in PBS at 30 °C for 15–30 min. Next, cells were washed twice with PBS and mounted on the slides. Finally, KB and Hep-2 cells were visualized using a digital microscope to examine DAPI (Excitation 375/28, Emission 460/50) and RFP (Excitation 530/40, Emission 605/55).

2.7. Detection of cellular reactive oxygen species (ROS)

To detect ROS levels, 2',7'-dichlorodihydrofluorescein diacetate (DCF-DA; Sigma-Aldrich) was used as a fluorescent probe. KB and Hep-2 cells were grown on coverslips and incubated in DMEM containing 60 µg/ml AC extract for the indicated time (0–12 h). After exposure to 625 nm IR for 1 h, the cells were stained with 25 µM DCF-DA, washed twice with PBS, and mounted on the slides. Finally, the cells were examined using a confocal microscope (Carl Zeiss, Oberkochen, Germany) with 488 nm excitation and 530 nm emission filters.

2.8. Flow cytometry

The apoptotic rates of KB and Hep-2 cells were examined using the Annexin V-FITC Apoptosis Detection Kit (Sigma-Aldrich), containing Annexin V-FITC Conjugate (Annexin V-FITC) and propidium iodide (PI) solution for analysis of apoptosis. Firstly, cells were divided into four groups: control, 625 nm IR, AC group, and AC with 625 nm IR groups. Each group of cells was then resuspended in 500 µl of 1×10^6 binding buffer at a concentration of 1×10^6 cells/ml in a plastic 12 × 75 mm test tube. Next, 5 µl of Annexin V-FITC Conjugate and 10 µl of PI

solution were added to each test tube and incubated at room temperature for 10 min in the dark. Finally, cell apoptosis analysis was performed by flow cytometry (Beckman-Coulter, Miami, USA).

2.9. Western blot analysis

The KB and Hep-2 cells were collected in lysis buffer, containing 150 mM NaCl, 50 mM Tris-HCl (pH 7.5), 1 mM EDTA, 1% NP-40, 1 mM PMSF, and 1% protease inhibitor cocktail. Samples containing equal amounts of protein were separated by 10% SDS-polyacrylamide gel and transferred to a polyvinylidene difluoride (PVDF) membrane (Merck KGaA, Darmstadt, Germany). The membrane was incubated with primary antibodies of proteins associated with apoptosis, including anti-PARP-1 (1:1000), anti-GAPDH (1:1000), and anti-Bax (1:1000) (Cell Signaling Technology, Danvers, USA) and anti-Bcl-2 (1:1000) (Santa Cruz Biotechnology, Dallas, USA). Anti-rabbit IgG (1:1000) and anti-mouse IgG (1:1000) (Santa Cruz Biotechnology) were used as secondary antibodies. Protein immunoreactivity was detected using the chemiluminescence detection kit (GE Healthcare, Little Chalfont, UK).

2.10. Statistical analysis

Data are expressed as the mean \pm standard deviation. All experiments were repeated at least three times and the differences between groups were evaluated by one-way ANOVA test. A p value $<$ 0.01 indicated statistical significance.

3. Results

3.1. Fluorescence screening

Supplementary data 2 (S2) shows the fluorescence intensity of 289 traditional plant extracts analyzed by fluorescence emission as a preliminary screen. As shown in Fig. 1, 13 plant extracts showed considerable fluorescence intensity and were selected as primary candidates. The fluorescence levels of HP were used as control. HP reached its maximal fluorescence value of 100,000 units at 500 μ g/ml. Some

plant extracts exhibited approximately comparable fluorescence levels to HP.

3.2. Screening of novel photosensitizers

To compare the photodynamic effects of 13 primary candidates, KB and Hep-2 cells were treated with different doses of the plant extracts with and without 625 nm IR and the cell viability assayed. The lethal concentration 50 (LC50) values were calculated by trend line analysis of the extracts with and without 625 nm IR. The differences between values obtained with and without 625 nm IR for each extract are arranged in descending order in Table 1. *Loranthi Ramulus* extract showed a difference of 141.7 in KB cells, but the difference was only 21.5 in Hep-2 cells. However, *Houttuyniae Herba* (HH) and AC extracts showed higher differences than the other extracts in both KB and Hep-2 cells. Therefore, HH and AC were chosen as our primary candidates.

3.3. Optimal PDT conditions for a novel photosensitizer

KB, Hep-2, and HaCaT cells were treated with HH and AC extracts (0–100 μ g/ml) with and without 625 nm IR. As shown in Fig. 2C, the survival rate of HaCaT cells in the HH with 625 nm IR group was less than 50% at 40 μ g/ml. In contrast, both the AC and AC with 625 nm IR groups showed a high stable survival rate of approximately 90% at 0–60 μ g/ml. For KB and Hep-2 cells, treatment with 60 μ g/ml AC extract showed significant differences in survival rates, with and without 625 nm IR (Fig. 2A and B). To determine the optimal AC treatment time in KB and Hep-2 cells, the fluorescence and ROS levels of AC were analyzed at a series of time points. KB and Hep-2 cells were treated with 60 μ g/ml AC extract for 0–12 h. As shown in Fig. 3, when KB and Hep-2 cells were treated with AC extract for 2 h, AC fluorescence began to accumulate in the cytosol. At 8 h of AC treatment, the strongest AC fluorescence was detected in both KB and Hep-2 cells. AC fluorescence decreased at 12 h of treatment. As shown in Fig. 4A and B, the green DCF-DA fluorescence also peaked at 8 h in KB and Hep-2 cells. In contrast, the green DCF-DA fluorescence was barely detected in HaCaT cells (Fig. 4A and B). Next, to determine the survival rate of KB, Hep-2,

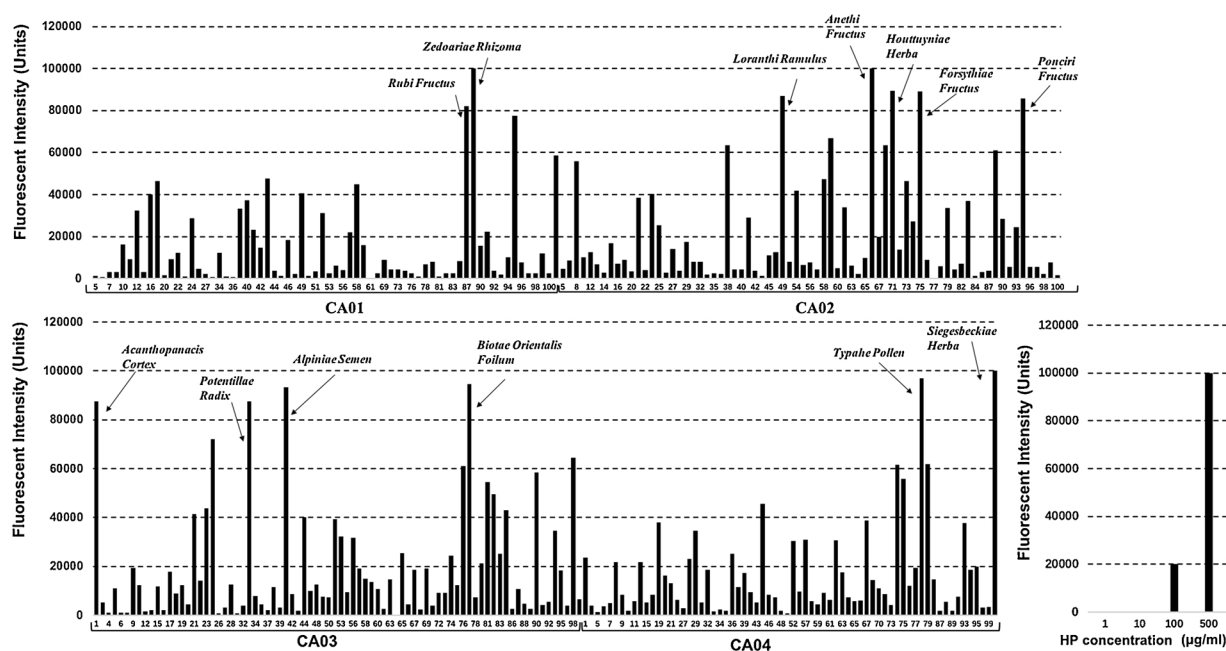


Fig. 1. 13 plant extracts showed strong fluorescence intensity. The fluorescence intensities of 289 plant extracts were compared to the maximum fluorescence of HP (100,000 units). The 13 plant extracts that were the closest to the maximum fluorescence value of HP were *Rubi Fructus*, *Zedoariae Rhizoma*, *Loranthi Ramulus*, *Anethi Fructus*, *Houttuyniae Herba*, *Forsythiae Fructus*, *Ponciri Fructus*, *Acanthopanax Cortex*, *Potentillae Radix*, *Alpiniae Semen*, *Biotae Orientalis Foilium*, *Typahe Pollen*, and *Siegesbeckiae Herba*.

Table 1

LC50 values of 13 plant extracts in KB and Hep-2 cells with and without 625 nm IR. The differences between the LC50 values obtained with and without 625 nm IR were arranged in descending order. (* $p < 0.01$, ** $p < 0.001$, *** $p < 0.0001$ plant extracts vs. plant extracts with 625 nm IR). “—”: the maximum concentration (500 $\mu\text{g/ml}$) did not reach the LC50. ND: Not detectable.

Plant extract	LC50 ($\mu\text{g/ml}$)				Plant extract	LC50 ($\mu\text{g/ml}$)			
	KB					Hep-2			
	Plant (A)	Plant + LED (B)	(A) – (B)	P-value		Plant (A)	Plant + LED (B)	(A) – (B)	P-value
<i>Loranthi Ramulus</i>	285.57	143.94	141.63	***	<i>Houttuyniae Herba</i>	316.32	62.98	253.34	***
<i>Houttuyniae Herba</i>	199.79	68.83	130.96	***	<i>Acanthopanax Cortex</i>	263.5	79.33	184.17	***
<i>Acanthopanax Cortex</i>	153.68	80.19	73.49	***	<i>Biotae Orientalis Foilum</i>	80.37	50.36	30.01	***
<i>Anethi Fructus</i>	150.48	103.75	46.73	***	<i>Siegesbeckiae Herba</i>	237.18	214.16	23.02	***
<i>Zedoariae Rhizoma</i>	165.16	124.52	40.64	***	<i>Loranthi Ramulus</i>	282	260.47	21.53	***
<i>Siegesbeckiae Herba</i>	216.15	184.87	31.28	***	<i>Typahe Pollen</i>	117.75	99.57	18.18	***
<i>Biotae Orientalis Foilum</i>	77.46	49.6	27.86	***	<i>Potentillae Radix</i>	111.49	98.75	12.74	**
<i>Ponciri Fructus</i>	250.74	231.26	19.48	***	<i>Zedoariae Rhizoma</i>	272.76	261.68	11.08	ND
<i>Potentillae Radix</i>	98.88	87.76	11.12	**	<i>Forsythiae Fructus</i>	76.33	77.69	-1.36	ND
<i>Typahe Pollen</i>	94.91	91.86	3.05	ND	<i>Anethi Fructus</i>	100.77	112.81	-12.04	***
<i>Alpiniae Semen</i>	76.48	75.46	1.02	ND	<i>Alpiniae Semen</i>	83.52	96.73	-13.21	***
<i>Forsythiae Fructus</i>	73.38	72.97	0.41	ND	<i>Ponciri Fructus</i>	261.14	290.36	-29.22	***
<i>Rubi Fructus</i>	—	—	—	ND	<i>Rubi Fructus</i>	—	—	—	ND

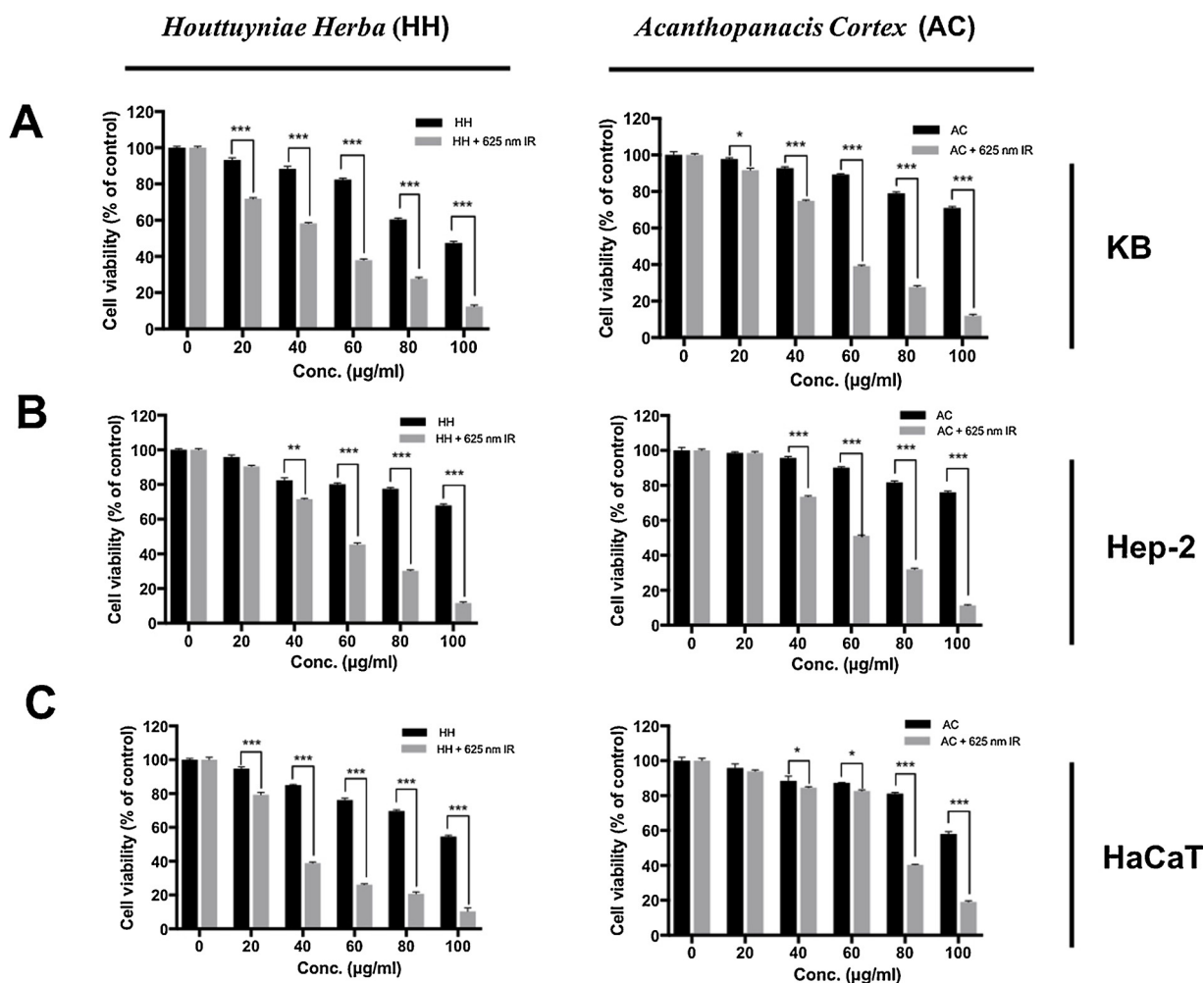


Fig. 2. Cell viability with and without 625 nm IR at various concentrations of HH and AC. KB, Hep-2 and HaCaT cells were treated with the indicated concentrations (0–100 $\mu\text{g/ml}$) of HH and AC for 12 h, followed by 625 nm IR for 1 h. The black bars represent HH or AC treatment alone, the light gray bars represent HH or AC with 625 nm IR treatment. (* $p < 0.1$, ** $p < 0.01$, *** $p < 0.001$ compared to the untreated control).

and HaCaT cells under the optimal AC treatment time and concentration, a cell viability assay was performed in a time-dependent and dose-dependent manner with and without 625 nm IR in KB, Hep-2, and HaCaT cells. As shown in Fig. 4C, AC extract with 625 nm IR induced

the most cell death in KB and Hep-2 cells at 8 h. In addition, the survival rate of KB cells was lower than that of Hep-2 cells and the survival rate of HaCaT cells was greater than 80% with 60 $\mu\text{g/ml}$ AC. As shown in Fig. 4D, the survival rates of KB and Hep-2 cells were both less than

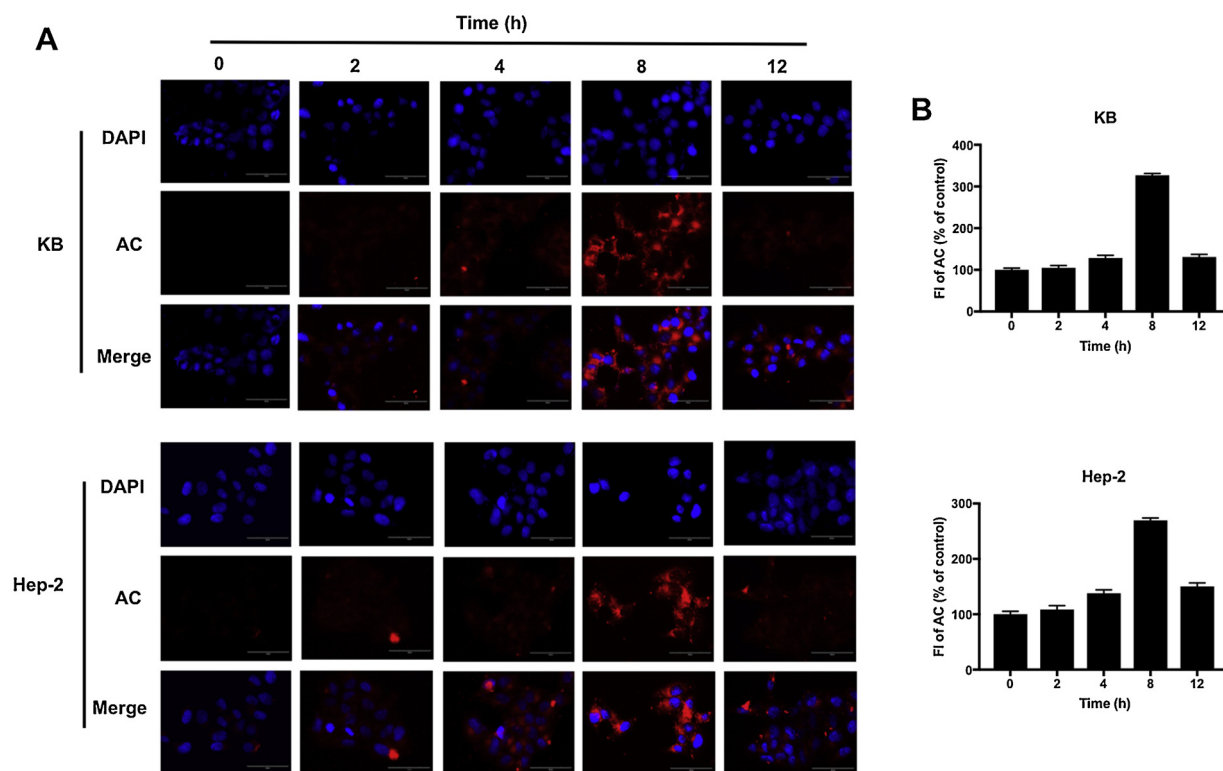


Fig. 3. Intracellular distribution of AC extract in KB and Hep-2 cells. AC fluorescence was observed by confocal microscopy to localize to the cytosol. The fluorescence intensity increased from 0 to 8 h. The AC fluorescence intensity (FI) in KB and Hep-2 cells was evaluated using CELENA[®]S Digital Imaging System. DAPI: fluorescent dye staining cell nuclei; AC: *Acanthopanax Cortex*.

35% with 60 $\mu\text{g}/\text{ml}$ AC for 8 h and 625 nm IR for 1 h. HaCaT cells also maintained a survival rate of more than 80% with 60 $\mu\text{g}/\text{ml}$ AC with or without 625 nm IR.

3.4. ROS generation with novel photosensitizer

To compare ROS levels in different conditions, KB and Hep-2 cells were divided into five groups: the control, 625 nm IR (625 nm IR for 1 h), AC (treated with 60 $\mu\text{g}/\text{ml}$ AC for 8 h), AC with 625 nm IR groups (treated with 60 $\mu\text{g}/\text{ml}$ AC for 8 h, followed by 625 nm IR for 1 h) and HP with 625 nm IR groups (treated with 2 μM for 8 h, followed by 625 nm IR for 1 h). As shown in Fig. 5, the control and 625 nm IR groups showed almost no green DCF-DA fluorescence. The AC group and HP with 625 nm IR group produced some slight green DCF-DA fluorescence. However, the AC with 625 nm IR group produced large amounts of green DCF-DA fluorescence and the signal was stronger than those of the other four groups.

3.5. AC with 625 nm IR induces cell apoptosis in KB and Hep-2 cells

To investigate whether AC with 625 nm IR induced apoptosis in KB and Hep-2 cells, Annexin V-FITC/PI flow cytometry and western blot analyses were performed. As shown in Fig. 6A and B, there was almost no difference between the control group and the 625 nm IR group, both in KB and Hep-2 cells, indicating that 625 nm IR treatment did not solely induce significant apoptosis. The AC only group induced a low level of apoptosis, with an apoptotic rate of approximately 10–20%. However, the apoptotic rate of the AC with 625 nm IR group reached 60–70%. The apoptosis-related protein expression of PARP-1, Bcl-2, and Bax was examined in the cell groups. In the AC with 625 nm IR group, expressed Bcl-2 protein was significantly down-regulated, the Bax protein was up-regulated, and the cleaved PARP-1 protein can be clearly seen in Fig. 6C.

4. Discussion

In the last 20 years, hematoporphyrin (HP) and its derivatives have been widely used as photosensitizers in the treatment of multiple carcinomas [23]. In order to develop novel photosensitizers, they should have comparable fluorescence intensity to the commercial product—HP. Therefore, the identification of novel photosensitizers with comparable fluorescence intensity to HP will have a positive effect on the development of novel photosensitizers. As shown in Fig. 1, the fluorescence intensities of 289 plant extracts (S2) were measured and 13 plant extracts with fluorescence intensity higher than 80,000 units—the intensity of HP, were selected. The 13 plant extracts were as follows: *Rubi Fructus*, *Zedoariae Rhizoma*, *Loranthi Ramulus*, *Anethi Fructus*, *HH*, *Forsythiae Fructus*, *Ponciri Fructus*, *AC*, *Potentillae Radix*, *Alpiniae Semen*, *Biotae Orientalis Folium*, *Typahe Pollen*, and *Siegesbeckiae Herba*. Fortunately, they are all readily available in eastern countries. Since these 13 extracts have similar fluorescence intensities to that of the commercial HP at 420 nm, they may have the potential to act as photosensitizers for photodynamic diagnosis (PDD). PDD often uses blue light to excite photosensitizer fluorescence for the detection of pathological tissue [24,25].

Next, we compared the effect of the 13 candidates that showed strong fluorescence with or without 625 nm IR, on cancer cells using cell viability assay (Table 1). The preliminary selection criteria for screening an ideal natural photosensitizer are as follows: the toxicity of the photosensitizer to cancer cells under 625 nm IR conditions; a high difference between the LC50 values of the photosensitizer with 625 nm IR and without 625 nm IR; simultaneous photodynamic toxic effect on KB and Hep-2 cells; and non-toxic effect of the photosensitizer on normal cells.

HH and AC extracts were found to satisfy the above criteria for 625 nm IR-induced cell death in KB and Hep-2 cells after determining the difference in LC50 values with and without 625 nm IR for the 13 plant extracts. Although HH extracts have antibacterial, anti-oxidative,

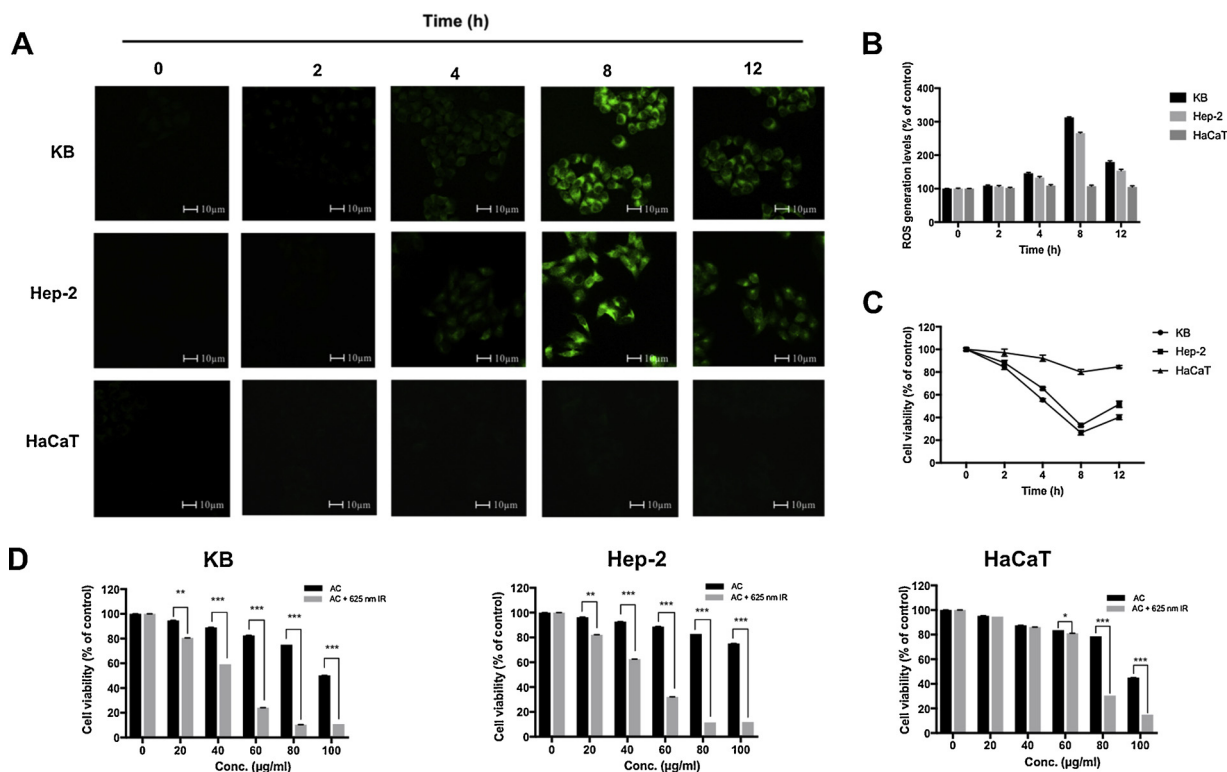


Fig. 4. Optimizing AC treatment conditions. (A) and (B) ROS levels in KB, Hep-2, and HaCaT cells treated with AC and 625 nm IR. Green DCF-DA fluorescence in the AC with 625 nm IR group was strongest at 8 h and the fluorescence intensity increased steadily from 0 to 8 h. HaCaT cells had barely detectable green DCF-DA fluorescence. The green DCF-DA fluorescence intensity in KB and Hep-2 cells was evaluated using ImageJ software. (C) KB, Hep-2, and HaCaT cells were treated with 60 µg/ml of AC for 0–12 h, followed by 625 nm IR for 1 h. The lowest survival rate in both KB and Hep-2 cells was at 8 h. At the same time, HaCaT cells maintained a high survival rate. (D) KB, Hep-2, and HaCaT cells were treated with the indicated concentrations (0–100 µg/ml) of AC for 8 h, followed by 625 nm IR for 1 h. Treatment 60 µg/ml of AC produced a satisfactory photodynamic effect. Black bars represent AC treatment alone, light gray bars represent AC with 625 nm IR treatment. (* $p < 0.1$, ** $p < 0.01$, *** $p < 0.001$ compared to the untreated control).

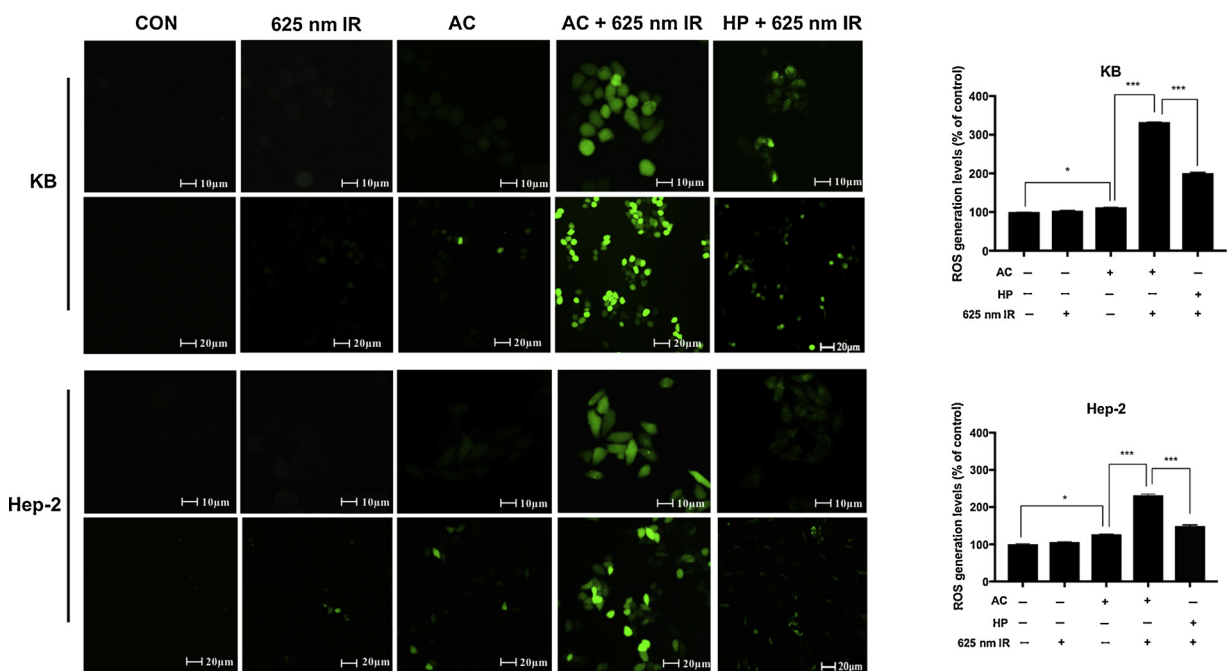


Fig. 5. ROS levels in five treatment groups of KB and Hep-2 cells. The AC with 625 nm IR group produced the strongest green DCF-DA fluorescence of the five treatment groups. The green DCF-DA fluorescence intensity in KB and Hep-2 cells was evaluated using ImageJ software (* $p < 0.1$, ** $p < 0.01$, *** $p < 0.001$ of the AC group compared to the AC with 625 nm IR group).

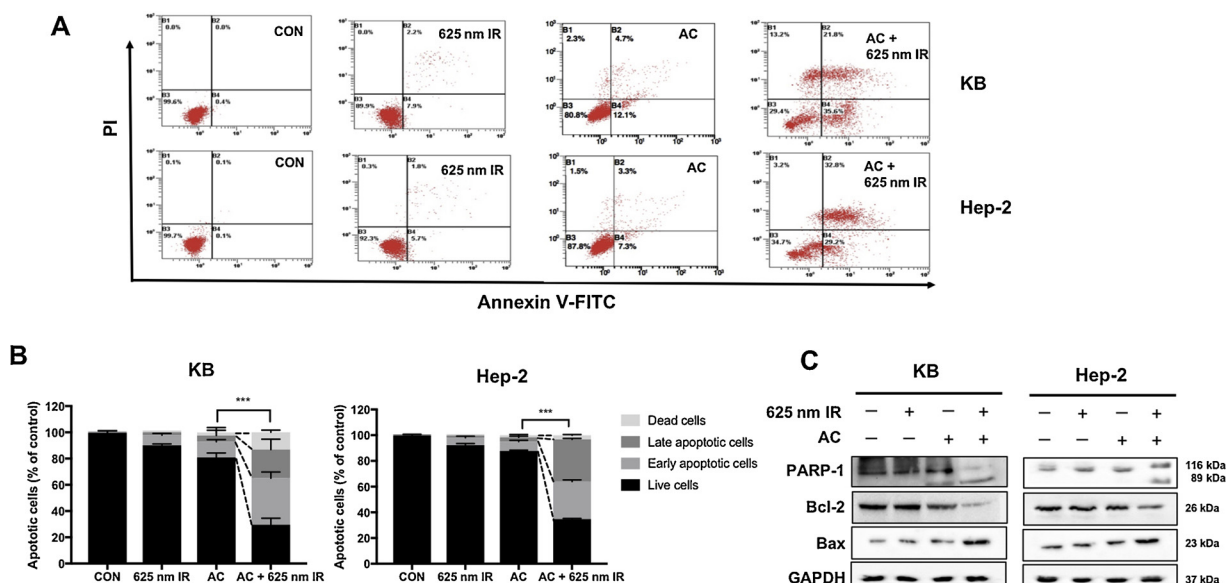


Fig. 6. AC with 625 nm IR induced apoptosis in KB and Hep-2 cells. (A) and (B), Annexin V-FITC/PI staining for apoptosis were analyzed by flow cytometry. Treatment with AC and 625 nm IR led to high levels of apoptosis in both KB and Hep-2 cells. The apoptosis rate of the AC with 625 nm IR group was compared to that of the AC group (* $p < 0.1$, ** $p < 0.01$, *** $p < 0.001$). (C) Western blot assay, expression levels of apoptosis-related proteins (Bcl-2, Bax, and PARP-1) in KB and Hep-2 cells.

and anti-cancer effects [26–28], also study reported that HH injection can cause adverse effects in patients [29]. Additionally, as shown in Fig. 2C, HH had significant photodynamic toxicity in HaCaT cells with and without 625 nm IR. In contrast, both AC and AC with 625 nm IR groups showed a high stable survival rate. AC refers to the barks of the roots and stem of *Acanthopanax sessiliflorus*, a plant of the Araliaceae family. Many chemical compounds were isolated from *Acanthopanax sessiliflorus*, including triterpenoid saponins, lignans, coumarins, and flavones [30–33]. Recently, studies have shown that the main coumarin component isolated from the bark of *A. senticosus* can inhibit ERK1/2 phosphorylation in hepatoma cell lines, inhibiting MMP-7 expression and cell invasion at a non-toxic level [34]. The polysaccharide extracted from *A. senticosus* has tumor suppressive effect on Croker sarcoma S80, liver cancer H22 and cervical cancer U4 cell lines [35]. In addition, a recent report showed that AC extract had a certain inhibitory effect on cell proliferation in multiple kinds of tumor in vitro and in vivo [36]. Treatment of KB and Hep-2 cells with 60 $\mu\text{g}/\text{ml}$ AC led to significant differences between the survival rates of groups with and without 625 nm IR as shown in Fig. 2A and B. Therefore, we suggest that AC extract is a potential novel natural photosensitizer against HNSCC.

In PDT, the intracellular distribution of photosensitizers is highly relevant to the outcomes of PDT [37]. In general, photosensitizers are transported into the cells in one of two ways: hydrophilic and anionic photosensitizers are internalized by endocytosis, mainly in lysosomes; lipophilic photosensitizers bind to low-density lipoproteins and their conjugates release the photosensitizer into the cytosol [38]. As shown in Fig. 3, AC extract gradually accumulated in the cytosol in a time-dependent manner and the fluorescence intensity lasted for over 8 h in both KB and Hep-2 cells. Since the mitochondria have high oxygen levels, ROS can be easily produced after the accumulation of the photosensitizer [39]. Moreover, in PDT, ROS generation can induce mitochondrial dysfunction, leading to cell death [40]. As shown in Fig. 4, KB and Hep-2 cells treated with 60 $\mu\text{g}/\text{ml}$ AC extract for 8 h and 625 nm IR for 1 h, had the strongest green DCF-DA fluorescence and lowest survival rate. In contrast, HaCaT cells did not produce significant ROS fluorescence and cell survival rate was maintained at more than 80%.

ROS production by cancer cells under PDT conditions leads to activation of the protein kinase pathway and releases many mediators responsible for the process of cell death, which may induce apoptosis or

necrosis [41]. As shown in Fig. 5, the ROS levels caused by AC extract with 625 nm IR were increased by approximately three fold compared to those with the AC extract alone in KB cells and by approximately two fold in Hep-2 cells. Also, the ROS level caused by AC extract with 625 nm IR was higher than that by HP with 625 nm IR in both KB and Hep-2 cells. Furthermore, as shown in Fig. 6A and B, KB and Hep-2 cells treated with AC extract with 625 nm IR showed high levels of apoptosis by Annexin V-FITC / PI flow cytometry analysis. In contrast, treatment with the AC extract alone did not result in significant apoptosis. The main function of mitochondria in the apoptotic signaling pathway is to release pro-apoptotic proteins, normally contained in the inter-membrane space, into the cytoplasm, triggering downstream apoptotic signaling pathways in the cytosol [42]. This release is controlled by the Bcl-2 family of proteins to activate the two pro-apoptotic members Bax and Bak [43]. As Bcl-2 transfection leads to overexpression of Bax, the release of cytosolic Bcl-2 can lead to overexpression of Bax [44]. As shown in Fig. 6C, PARP-1 was activated to form a cleavage protein, Bcl-2 expression was down-regulated, and Bax expression was up-regulated. When inducing apoptosis, the up-regulated expression of Bax was positively correlated with the degradation of PARP-1 protein. Therefore, it can be speculated that AC extract acting as a novel photosensitizer in PDT could produce ROS and trigger the apoptotic signaling pathway of KB and Hep-2 cells.

In this study, AC extract has similar fluorescence intensity to that of commercial HP, at 420 nm. Hence, AC extract plus 625 nm IR could enhance the PDT effect, induce ROS generation, and trigger apoptotic signaling pathways in KB and Hep-2 cells. Our study demonstrated by means of cell viability assays, ROS generation, Annexin V-FITC / PI flow cytometry analysis, and western blotting in vitro, that cell death rate due to PDT was perceptibly higher than those of other single therapeutic approaches. Therefore, we suggest that AC extract may be used as a novel photosensitizer for PDT in HNSCC. Furthermore, AC extract can be used as either a photosensitizer for PDD or a photosensitizer for PDT under different light sources. Finally, this study is the first to report the use of AC extract as a photosensitizer, hence further investigation is required to validate the results of this study.

Ethical approval

This study did not involve human participants or animals.

Conflict of interest

The authors declare that they have no conflicts of interest.

Acknowledgments

This work was supported by National Research Foundation of Korea (NRF) grants (NRF-2016R1D1A1B03930314 and NRF-2016R1D1A1B03931467) funded by the Korean government.

Appendix A. Supplementary data

Supplementary material related to this article can be found, in the online version, at doi:<https://doi.org/10.1016/j.pdpdt.2019.02.020>.

References

- [1] A.K. Dhull, R. Atri, R. Dhankhar, A.K. Chauhan, V. Kaushal, Major risk factors in head and neck cancer: a retrospective analysis of 12-year experiences, *World J. Oncol.* 9 (2018) 80–84.
- [2] U. Sunar, Monitoring photodynamic therapy of head and neck malignancies with optical spectroscopies, *World J. Clin. Cases* 1 (2013) 96–105.
- [3] J. Menzin, L.M. Lines, L.N. Manning, The economics of squamous cell carcinoma of the head and neck, *Curr. Opin. Otolaryngol. Head Neck Surg.* 15 (2007) 68–73.
- [4] J.Y. Liu, P.Z. Zhou, J.L. Ma, X. Jia, Trifluoromethyl boron dipyrromethene derivatives as potential photosensitizers for photodynamic therapy, *Molecules* 23 (2018) pii: E458.
- [5] C. Zhang, J.Q. Jiang, Current status and prospect of photodynamic therapy in laryngeal diseases, *Zhonghua er bi yan hou tou jing wai ke za zhi* 53 (2018) 306–311.
- [6] W.M. Sharman, C.M. Allen, J.E. van Lier, Role of activated oxygen species in photodynamic therapy, *Methods Enzymol.* 319 (2000) 376–400.
- [7] R.R. Allison, G.H. Downie, R. Cuenca, X.H. Hu, C.J. Childs, et al., Photosensitizers in clinical PDT, *Photodiagnosis Photodyn. Ther.* 1 (2004) 27–42.
- [8] E.D. Sternberg, D. Dolphin, C. Brückner, Porphyrin-based photosensitizers for use in photodynamic therapy, *Tetrahedron* 54 (1998) 4151–4202.
- [9] J.M. Dąbrowski, M. Krzykawska, L.G. Arnaut, M.M. Pereira, C.J. Monteiro, et al., Tissue uptake study and photodynamic therapy of melanoma-bearing mice with a nontoxic, effective chlorin, *Chemmedchem* 6 (2011) 1715–1726.
- [10] D. Lafont, Y. Zorlu, H. Savoie, F. Albrieux, V. Ahsen, et al., Monoglycoconjugated phthalocyanines: effect of sugar and linkage on photodynamic activity, *Photodiagnosis Photodyn. Ther.* 10 (2013) 252–259.
- [11] B.O. Sun, W. Li, N. Liu, Curative effect of the recent photofrin photodynamic adjuvant treatment on young patients with advanced colorectal cancer, *Oncol. Lett.* 11 (2016) 2071–2074.
- [12] S. Toratani, R. Tani, T. Kanda, K. Koizumi, Y. Yoshioka, T. Okamoto, Photodynamic therapy using Photofrin and excimer dye laser treatment for superficial oral squamous cell carcinomas with long-term follow up, *Photodiagnosis Photodyn. Ther.* 14 (2016) 104–110.
- [13] L. Liang, S. Xie, L. Jiang, H. Jin, S. Li, J. Liu, The Combined effects of hematoporphyrin monomethyl ether-SDT and doxorubicin on the proliferation of QBC939 cell lines, *Ultrasound Med. Biol.* 39 (2013) 146–160.
- [14] B.B. Mishra, V.K. Tiwari, Natural products: an evolving role in future drug discovery, *Eur. J. Med. Chem.* 46 (2011) 4769–4807.
- [15] M. Fadel, K. Kassab, D.A. Abd El Fadeel, M. Nasr, N.M. El Ghoubari, Comparative enhancement of curcumin cytotoxic photodynamic activity by nanoliposomes and gold nanoparticles with pharmacological appraisal in HepG2 cancer cells and Erlich solid tumor model, *Drug Dev. Ind. Pharm.* 44 (2018) 1809–1816.
- [16] Y.Q. Liu, P.S. Meng, H.C. Zhang, X. Liu, M.X. Wang, W.W. Cao, et al., Inhibitory effect of aloe emodin mediated photodynamic therapy on human oral mucosa carcinoma in vitro and in vivo, *Biomed. Pharmacother.* 97 (2018) 697–707.
- [17] H.D. Lin, K.T. Li, Q.Q. Duan, Q. Chen, S. Tian, et al., The effect of aloe-emodin-induced photodynamic activity on the apoptosis of human gastric cancer cells: a pilot study, *Oncol. Lett.* 13 (2017) 3431–3436.
- [18] P. Agostinis, K. Berg, K.A. Cengel, T.H. Foster, A.W. Girotti, et al., Photodynamic therapy of cancer: an update, *CA Cancer J. Clin.* 61 (2011) 250–281.
- [19] S. Bharathiraja, H. Seo, P. Manivasagan, M. Santha Moorthy, S. Park, et al., In vitro photodynamic effect of phycocyanin against breast Cancer cells, *Molecules* 21 (2016) pii: E1470.
- [20] H.R. Van, J.P. Marijnissen, W.J. Kort, P.E. Zondervan, O.T. Terpstra, et al., Interstitial photodynamic therapy in a rat liver metastasis model, *Br. J. Cancer* 66 (1992) 1005–1014.
- [21] V.G. Wilson, Growth and differentiation of HaCaT keratinocytes, *Methods Mol. Biol.* 1195 (2014) 33–41.
- [22] H. Cho, H. Zheng, Q. Sun, S. Shi, O. Kim, et al., Development of novel photosensitizer using the *Buddleja officinalis* extract for head and neck cancer, *Evid. Based Complement. Altern. Med.* 2018 (2018) 1–10.
- [23] J. Kou, D. Dou, L. Yang, Porphyrin photosensitizers in photodynamic therapy and its applications, *Oncotarget* 8 (2017) 81591–81603.
- [24] K. Shimizu, M. Nitta, T. Komori, T. Maruyama, T. Yasuda, Y. Fujii, et al., Intraoperative photodynamic diagnosis using talaporfin sodium simultaneously applied for photodynamic therapy against malignant glioma: a prospective clinical study, *Front. Neurol.* 9 (2018) 24.
- [25] S.P. Lerner, A. Goh, Novel endoscopic diagnosis for bladder cancer, *Cancer* 121 (2) (2015) 169–178.
- [26] J. Fu, L. Dai, Z. Lin, H. Lu, *Houttuynia cordata* thunb: a review of phytochemistry and pharmacology and quality control, *Chin. Med.* 4 (2013) 101–123.
- [27] K.C. Lai, Y.J. Chiu, Y.J. Tang, K.L. Lin, J.H. Chiang, et al., *Houttuynia cordata* Thunb extract inhibits cell growth and induces apoptosis in human primary colorectal cancer cells, *Anticancer Res.* 30 (2010) 3549–3556.
- [28] Y.Y. Chen, J.F. Liu, C.M. Chen, P.Y. Chao, T.J. Chang, A study of the antioxidative and antimutagenic effects of *Houttuynia cordata* Thunb. using an oxidized frying oil-fred model, *J. Nutr. Sci. Vitaminol.* 49 (2003) 327–333.
- [29] Z.X. Bian, H.Y. Tian, L. Gao, H.C. Shang, T.X. Wu, et al., Improving reporting of adverse events and adverse drug reactions following injections of Chinese materia medica, *J. Evid. Med.* 3 (2010) 5–10.
- [30] Z.F. Li, Z.H. Wu, G. Chen, Q.H. Zhang, Y.H. Pei, Two new compounds from *Acanthopanax senticosus* harms, *J. Asian Nat. Prod. Res.* 11 (2009) 716–719.
- [31] W. Jiang, W. Li, L. Han, L. Liu, Q. Zhang, S. Zhang, et al., Biologically active triterpenoid saponins from *Acanthopanax senticosus*, *J. Nat. Prod.* 69 (2006) 1577–1581.
- [32] J. Ryu, D. Son, J. Kang, H.S. Kim, B.K. Kim, S. Li, A benzenoid from the stem of *Acanthopanax senticosus*, *Arch. Pharm. Res.* 27 (2004) 912–914.
- [33] Y. Wei, T.Y. Zhang, K.Y. Wu, Separation of eleutheroside E from crude extract of *Radix Acanthopanax Senticosus* by analytical and preparative high-speed counter-current chromatography, *Chin. J. Chromatogr.* 20 (2002) 543–545.
- [34] T. Yamazaki, T. Tokiwa, Isofraxidin, a coumarin component from *Acanthopanax senticosus*, inhibits matrix metalloproteinase-7 expression and cell invasion of human hepatoma cells, *Biol. Pharm. Bull.* 33 (2010) 1716–1722.
- [35] Q. Meng, J. Pan, Y. Liu, L. Chen, Y. Ren, Anti-tumour effects of polysaccharide extracted from *Acanthopanax senticosus* and cell-mediated immunity, *Exp. Ther. Med.* 15 (2018) 1694–1701.
- [36] B.E. Shan, Q.X. Li, W.J. Liang, Experimental study on anti-tumor effects of cortex *Acanthopanax senticosus* in vivo and in vitro, *Chin. J. Integr. Tradit. West. Med.* 24 (2004) 55–58.
- [37] B. Chen, B.W. Pogue, P.J. Hoopes, T. Hasan, Vascular and cellular targeting for photodynamic therapy, *Crit. Rev. Eukaryot. Gene Expr.* 16 (2006) 279–305.
- [38] K. Berg, J. Moan, Lysosomes and microtubules as targets for photochemotherapy of cancer, *Photochem. Photobiol.* 65 (2010) 403–409.
- [39] S.M. Mahalingam, J.D. Ordaz, P.S. Low, Targeting of a photosensitizer to the mitochondrion enhances the potency of photodynamic therapy, *ACS Omega* 3 (2018) 6066–6074.
- [40] H. Ito, H. Matsui, Mitochondrial reactive oxygen species and photodynamic therapy, *Laser Ther.* 25 (2016) 193–199.
- [41] M. Pawel, Y. Anastasia, G.B. Kharkwal, M.R. Hamblin, Cell death pathways in photodynamic therapy of Cancer, *Cancers* 3 (2011) 2516–2539.
- [42] T.J. Vilches, Understanding cell death: a challenge for biomedicine, *An. R. Acad. Nac. Med. (Madr.)* 122 (2005) 631–659.
- [43] J.M. Dąbrowski, L.G. Arnaut, Photodynamic therapy (PDT) of cancer: from local to systemic treatment, *Photochem. Photobiol. Sci.* 14 (2015) 1765–1780.
- [44] D. Carmonagutierrez, T. Eisenberg, S. Büttner, C. Meisinger, G. Kroemer, et al., Apoptosis in yeast: triggers, pathways, subroutines, *Cell Death Differ.* 17 (2010) 763–773.